

Rain initiation time in turbulent warm clouds

GREGORY FALKOVICH

Institute for Advanced Study, Princeton and Weizmann Institute of Science, Israel

MIKHAIL G. STEPANOV

Institute for Advanced Study, Princeton and Weizmann Institute of Science, Israel

MARIJA VUCELJA

Belgrade University, Yugoslavia and Weizmann Institute of Science, Israel

ABSTRACT

We present a mean-field model that describes droplet growth due to condensation and collisions and droplet loss due to fallout. The model allows for an effective numerical simulation. We study how the rain initiation time depends on different parameters. We also present a simple model that allows one to estimate the rain initiation time for turbulent clouds with an inhomogeneous concentration of cloud condensation nuclei. In particular, we show that over-seeding even a part of a cloud by small hygroscopic nuclei one can substantially delay the onset of precipitation.

1. Introduction

Droplets start growing by vapor condensation on cloud condensation nuclei (CCN) which are typically submicron-size particles. In warm clouds, coalescence due to collisions contributes the growth until the raindrops (generally exceeding millimeters) fall out of the cloud, see e.g. Pruppacher and Klett (1997). Those processes can be modelled by the equation for the local distribution of droplets over sizes, $n(a, t, \mathbf{r}) = n(a)$ and the mass content of the water vapor, $M(t, \mathbf{r})$:

$$\frac{\partial n(a)}{\partial t} + (\mathbf{v} \cdot \nabla)n = -\frac{\kappa s M}{\rho_0} \frac{\partial}{\partial a} \frac{n(a)}{a} \quad (1)$$

$$+ \int da' \left[\frac{K(a', a'')n(a')n(a'')}{2(a''/a)^2} - K(a', a)n(a')n(a) \right],$$

$$\frac{\partial M}{\partial t} + (\mathbf{v} \cdot \nabla)M - \kappa \Delta M = -4\pi s \rho_0 \kappa \int a n(a) da. \quad (2)$$

Here a is the droplet radius, t is time and \mathbf{r} is the coordinate in space. The first term in the right-hand

side of (1) is due to condensation which (for not very large droplets) changes the droplet size a according to $da^2/dt = \kappa s M/\rho_0$ where κ is vapor diffusivity, s is the degree of supersaturation and $\rho_0 = 10^3 \text{ kg} \cdot \text{m}^{-3}$ is the density of liquid water. The time needed for condensation to grow a droplet of size a is generally proportional to a^2 . The second term in the rhs of (1) describes coalescence due to collisions, here $a'' = (a^3 - a'^3)^{1/3}$ is the size of the droplet that produces the droplet of size a upon coalescence with the droplet of size a' . The collision kernel is the product of the target area and the relative velocity of droplets upon the contact: $K(a, a') \simeq \pi(a+a')^2 \Delta v$. According to the recent precise measurements (Beard et al, 2002) the coalescence efficiency of the droplets in the relevant intervals is likely to be greater than 0.95 we put it unity in our calculations. Collisions change the concentration $n(a)$ on a timescale of order $1/K(a, a_1)n(a_1)$ where collision kernel K is a fast growing function of droplet sizes.

Since condensation slows down and coalescence accelerates as the size of droplets grow then one can introduce a crossover scale a_* , determined by $K(a_*)n \simeq \kappa s M/\rho_0 a_*^2$. The growth up to the crossover scale is mainly due to condensation while coalescence provides

Corresponding author address:

G. Falkovich, Physics of Complex Systems, Weizmann Institute of Science, Rehovot 76100 Israel, gregory.falkovich@weizmann.ac.il

for the further growth. The crossover scale a_* depends on n and is typically in tens of microns (see below).

To describe the six unknown functions, n, M, s, \mathbf{v} , one must also add the equation that describes the temperature change (that determines s) and the Navier-Stokes equation for the velocity. Such system cannot be possible solved numerically with any meaningful resolution neither presently nor in a foreseeable future. The main problem is a very complicated spatial structure of the fields involved particularly due to cloud turbulence. Our aim in this paper is to formulate some mean-field model which does not contain spatial arguments at all. The requirements to this model is that it must give the correct qualitative relations between the parameters and reasonable quantitative description (at least within the order of magnitude) of the real-world timescales. According to the two basic phenomena involved (condensation and collisions), the main problems in space-averaging the equations are related to the proper description of the two phenomena: mixing and diffusion of water vapor and the influence of cloud turbulence on collisions. We address them in Sections 4 and 3 respectively. We use the model to study the evolution of $n(a, t)$ starting from sub-micron sizes all the way to the moment when droplet fallout significantly decreases the water content in the cloud. We shall call this moment the rain initiation time and we study how that time depends on initial vapor content and CCN concentration and on the level of air turbulence.

2. Growth by gravitational collisions

For the parameters typical for warm precipitating clouds ($sM/\rho_0 = 10^{-8} \div 10^{-9}$ and $n = 10^6 \div 10^9 \text{ m}^{-3}$), collisions are negligible for micron-size droplets (Pruppacher and Klett 1997). For droplets larger than couple of microns, Brownian motion can be neglected and the collision kernel in a still air is due to gravitational settling:

$$K_g(a, a') = \pi(a+a')^2 E(a, a') |u_g(a) - u_g(a')|. \quad (3)$$

The fall velocity u_g is obtained from the balance of gravity force $4\pi g \rho_0 a^3/3$ and the friction $F(u_g, a)$. The friction force depends on the Reynolds number of the flow around the droplet, $Re_a \equiv u_g a/\nu$. When Re_a is of order unity or less, $F = 6\pi\nu\rho a u_g$ and $u_g = g\tau$ where ρ is the air density and $\tau = (2/9)(\rho_0/\rho)(a^2/\nu)$ is called Stokes time. We use $u_g = g\tau$ for $a < 40\mu\text{m}$ and take $u_g(a)$ from the measurements of Gunn and Kinzer (1949) for $a > 50\mu\text{m}$ with a smooth interpolation for $40\mu\text{m} < a < 50\mu\text{m}$ as shown in Fig 1. The dotted straight lines have slopes 2, 1, 1/2. One can see that $u_g \propto a^2$ at $a < 40\mu\text{m}$. There is an intermediate interval with an approximately linear law $u_g \propto a$ for

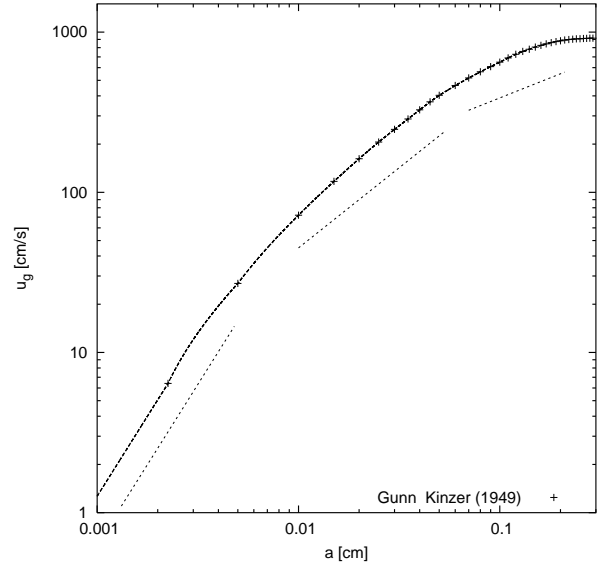


FIG. 1. Terminal fall velocity.

$40\mu\text{m} < a < 400\mu\text{m}$. When $Re_a \gg 1$ one may expect $F \propto \rho a^2 u_g^2$ as long as droplet remains spherical; that gives $u_g \propto \sqrt{ag\rho_0/\rho}$. Square-root law can be distinguished between $400\mu\text{m}$ and 1mm while the growth of $u_g(a)$ saturates at larger a due to shape distortions. Hydrodynamic interaction between approaching droplets is accounted in K_g by the collision efficiency E , which values we take from Pinsky et al (2001) at the 750 mbar altitude.

It is of practical use to be able to predict the time left before rain starts given the knowledge of droplet distribution at a given instant. Such distributions can be measured with high accuracy by optical and other methods. Drop size distributions measured in many different types of clouds under a variety of meteorological conditions often exhibit a characteristic shape (Pruppacher and Klett, 1997). Generally the concentration rises sharply from low value maximum, and then decreases gently toward larger sizes, causing the distribution to be positively skewed with a long tail toward the larger sizes. We approximate such a shape with half-Gaussian $\theta(a - a_0) \exp(-(a - a_0)^2/2\sigma^2)$ where θ is a step function. We thus characterize the distribution by two parameters: the mean position P and the width σ . Since we mainly consider narrow initial distributions ($\sigma \ll P$), the rain initiation time does not depend substantially on the initial shape. We start from purely gravitational collisions in a still air that is solve the space-homogenous version of (1) with no condensation term:

$$\frac{\partial n(a)}{\partial t} = -n(a) \frac{u_g(a)}{L} \quad (4)$$

$$+ \int da' \left[\frac{K_g(a', a'')n(a')n(a'')}{2(a''/a)^2} - K_g(a', a)n(a')n(a) \right].$$

The first term in the rhs of (4) models the loss of droplets falling with the settling velocity u_g from the cloud of the vertical size L . Since L are generally very large (from hundreds meters to kilometers) and $u_g(a)$ grows with a (see Fig. 1 below), fallout is relevant only for sufficiently large drops (called raindrops) with sizes millimeter or more. The collision (Smoluchowsky) term describes the propagation of distribution towards large sizes. The asymptotic law of propagation depends on the scaling of $K_g(a, a')$. If the collision kernel is a homogeneous function of degree α [that is $K_g(\xi a, \xi a') = \xi^\alpha K_g(a, a')$] one can show that for α larger/smaller than three the propagation is accelerating/decelerating while for $\alpha = 3$ it is exponential $\ln a \propto t$ (see van Dongen and Ernst 1988; Zakharov et al 1991). Our numerics show, however, that the intervals of sizes a where α is approximately a constant are too short for definite self-similarity of the propagation to form both for narrow and wide initial distributions. This is due to complexity of both functions, $u_g(a)$ and $E(a, a')$. We thus focus on the most salient feature of the propagation, namely study how the amount of water left in the cloud, W , depends on time. The decrease of that amount is due to a concerted action of collisions producing large drops and fallout.

The droplets radii space was discretized, i.e. the droplets size distribution $n(a, t)$ was presented as the set of concentrations $n_i(t)$ of droplets with radius a_i . The total mass of vapor and water in droplets is conserved in our calculations. The grid of radii was taken approximately exponential at sizes that are much larger than the size of initial condensation nuclei, with 256 points in unit interval of natural logarithm. The collision term in Smoluchowsky equation was treated as follows: let the radius $(a_i^3 + a_j^3)^{1/3}$ of the droplet resulted from merging of the two with radii a_i and a_j to be in between of two radii a_k and a_{k+1} from the grid. Then the collision results in decreasing of n_i and n_j by quantity dN that is determined by the collision kernel, while the concentrations n_k and n_{k+1} are increased in such a way that sum of their change is dN and the whole amount of water in droplets is conserved in coalescence:

$$\begin{aligned} \delta n_i &= \delta n_j = -dN = -\delta n_k - \delta n_{k+1}, \\ a_k^3 \delta n_k + a_{k+1}^3 \delta n_{k+1} &= (a_i^3 + a_j^3) dN, \\ \delta n_{k+1} &= dN (a_i^3 + a_j^3 - a_k^3) / (a_{k+1}^3 - a_k^3), \\ \delta n_k &= dN (a_{k+1}^3 - a_i^3 - a_j^3) / (a_{k+1}^3 - a_k^3). \end{aligned} \quad (5)$$

The total amount of water (the sum of the part that left and remained in the cloud) was a conserved quantity, up to 10^{-6} accuracy, during the whole simulation.

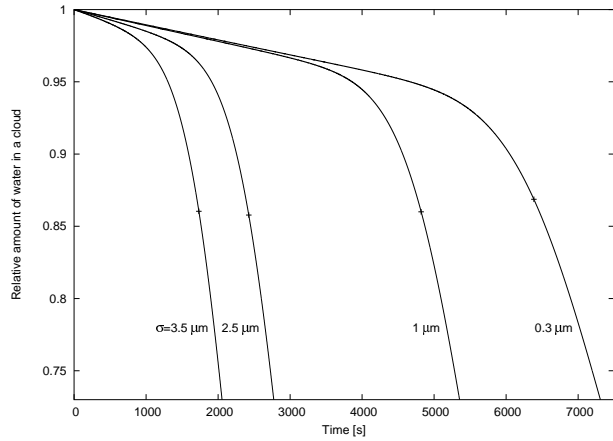


FIG. 2. Fraction of water left in the cloud as a function of time. $P = 13 \mu\text{m}$.

Note that our scheme automatically keeps the numbers positive: if dN is greater than either n_i or n_j , then we choose $dN = \min\{n_i, n_j\}$, so that n_i and n_j are also not negative after every elementary collision process. Let us stress that our scheme is conservative both in mass and number of droplets (comparing to the non-conservative scheme of Berry and Reinhardt, 1974 and the scheme of Bott, 1998 which was conservative only in mass and needed special choice of the time step to keep positivity). The minimal time step needed for our calculations was estimated from characteristic timescales of our problem to be 0.1 s. We have checked that the decrease of the time step below $dt = 0.05$ s does not change the results, the figures below all correspond to that dt .

The graphs $W(t)$ are shown at Figs 2 and 3 (for $L = 2$ km) and they are qualitatively the same both for narrow and wide initial distributions. At the initial stage, W decreases slowly due to the loss of drizzle. After large raindrops appear, loss accelerates. At every curve, the star marks the moment when respective d^2W/dt^2 are maximal. After that moment, the cloud loses water fast so it is natural to take t_* as the beginning of rain. Figure 4 shows how the mass distribution over sizes, $m(a) \propto a^3 n(a)$ evolves with time. One can see the appearance of secondary peaks and distribution propagating to large a . The moment t_* seems to correspond to the highest value of the envelope of the curves $m(a, t)$ of the coalescence-produced drops. One can see from Figure 4 that the peak at mass distribution is around 200 microns and most of the droplets are below 500 microns at $t = t_*$. The same character of the evolution $W(t)$ can be seen in the next section for the *ab initio* simulations of (1,2).

The rain initiation time t_* defined in that way is

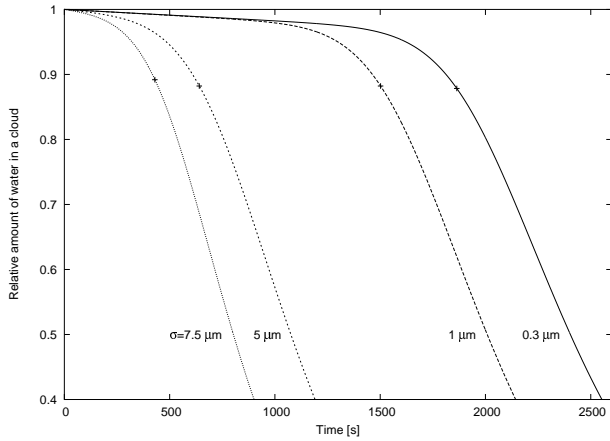


FIG. 3. Fraction of water left in the cloud as a function of time. $P = 16 \mu\text{m}$.

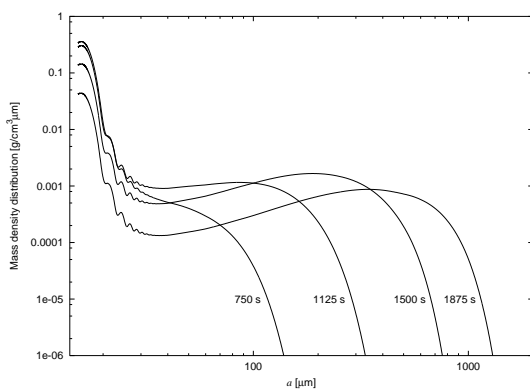


FIG. 4. Mass density of water, $t_* \simeq 1500 \text{ s}$.

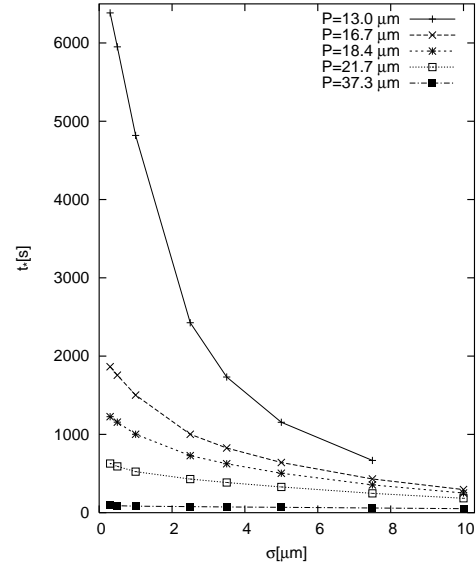


FIG. 5. Rain initiation time as function of the width of initial distribution σ for different initial positions P .

presented in Figures 5 and 6 against the width and the position of the initial distribution. Note the dramatic increase in t_* with decreasing σ for $P = 13 \mu\text{m}$. The mean droplet size $P = 14 \mu\text{m}$ is sometimes empirically introduced as the minimal size required for the onset of precipitation (Rosenfeld and Gutman 1994). Figures 5 and 6 support that observation, they indeed show that t_* grows fast when P decreases below that size but only for very narrow initial distributions and of course there is no clear-cut threshold as $t_*(P)$ is a smooth (though steep) function. The timescales (from tens of minutes to hours) are in agreement with the data obtained before (see Pruppacher and Klett, 1997, Chapter 15; and Seinfeld, J. and S.Pandis, 1998, Chapter 15 and the references therein). Figure 6 also shows that for $15 \mu\text{m} \lesssim P$, the function $t_*(P)$ can be well-approximated by a power law $t_* \propto P^{-\gamma}$ with $\gamma \approx 3$. The rain initiation time depends on the cloud vertical size almost logarithmically as shown in Fig. 7, we do not have an explanation for this functional form.

Here we treated the position and the width of the distribution as given at the beginning of the collision stage. But of course the distribution is itself a product of condensation stage so we now turn to the consideration of the full condensation-collision model.

3. Condensation and collisions

We consider now the space-homogeneous system

$$\frac{\partial n(a)}{\partial t} = -\frac{\kappa s M}{\rho_0} \frac{\partial}{\partial a} \frac{n(a)}{a} - n(a) \frac{u_g(a)}{L} \quad (6)$$

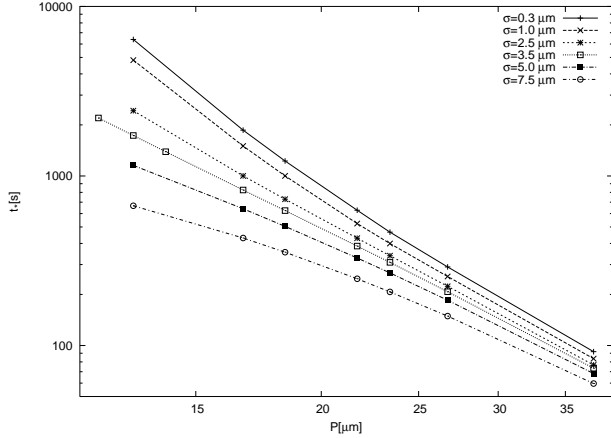


FIG. 6. Rain initiation time as function of the position of the initial distribution.

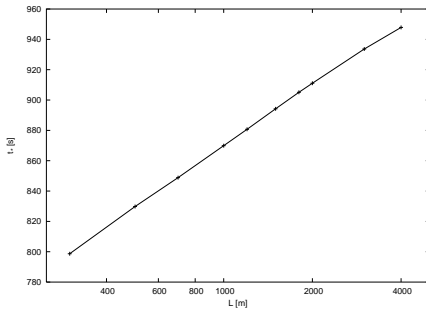


FIG. 7. Rain initiation time as function of the cloud vertical size.

$$+ \int da' \left[\frac{K(a', a'')n(a')n(a'')}{2(a''/a)^2} - K(a', a)n(a')n(a) \right],$$

$$\frac{\partial M}{\partial t} = -4\pi s \rho_0 \kappa \int an(a)da. \quad (7)$$

If one substitutes here gravitational and Brownian collision kernels (taken, e.g. from Pruppacher and Klett 1997) and start from $n = 10^7 \div 10^8 \text{ m}^{-3}$ sub-micron droplets growing in a medium with $sM/\rho_0 = 10^{-8} \div 10^{-9}$ then (6,7) give unrealistically large rain initiation time. The reason for that is well-known: during the condensation stage, the distribution shifts to larger sizes while keeping its small width over a^2 . For narrow distributions, gravitational collisions are suppressed (since all droplets fall with close velocities) as we have seen in the previous section. Collisions of droplets with similar sizes are provided by an inhomogeneous air flow. The velocity gradient λ provides for the kernel $K_s = \lambda(a+a')^3$ derived in Saffman and Turner (1956). However, typical velocity gradients in the air turbulence ($\lambda \simeq 10-30 \text{ s}^{-1}$) also do not provide enough collisions (see e.g. Pruppacher and Klett 1997; Jonas 1996; Vaillancourt and Yau 2000, and the referenced therein). Regular vertical inhomogeneity of supersaturation due to temperature profile does not broaden $n(a)$ much even with the account of turbulence-induced random fluctuations (Korolev 1995; Turitsyn 2003). Spatial inhomogeneities in vapor content M due to mixing of humid and dry air still remains a controversial subject (see. e.g Pruppacher and Klett 1997; Baker et al, 1980) and probably can be neglected in cloud cores. We address the turbulent mixing of vapor in Section 4 considering partially seeded clouds. We address the turbulent mixing of vapour in Section 4 considering partially seeded clouds. As far as collisions are concerned, the main effect of spatial inhomogeneities seems to be the effect of preferential concentration that is of turbulence-induced fluctuations in droplets concentration (see Maxey 1987; Squires and Eaton 1991; Sundaram and Collins 1997; Reade and Collins 2000; Grits et al 2000; Shaw et al 1998; Kostinski and Shaw 2001, and the references therein). We use here the results of the recent theory by Falkovich et al (2002). Namely, we multiply the Saffman-Turner collision kernel K_s by the enhancement factor $\langle n_1 n_2 \rangle / \langle n_1 \rangle \langle n_2 \rangle$ (which accounts for the effects of inertia and gravity in a turbulent flow) and add the collision kernel due to the so-called sling effect (droplets shot out of air vortices with too high centrifugal acceleration), see Falkovich et al (2002) and Falkovich and Pumir (2004) for the details. The total collision kernel due to turbulence normalized by the homogeneous expression $8\lambda a^3$ factor is presented in Fig. 8 for $Re = 10^6$. We see that role of concentration inhomogeneities can be substantial in the interval between 30 and 60 μm .

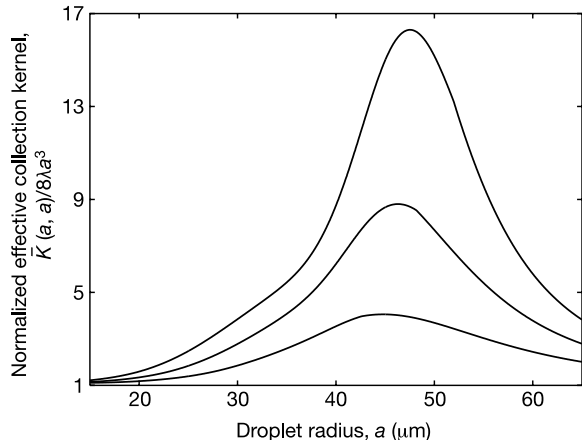


FIG. 8. Turbulence collision kernel normalized by $8\lambda a^3$ for equal-size droplets at $\text{Re} = 10^6$. From bottom to top, $\lambda = 10, 15$ and 20 s^{-1} .

The role of sling effect is not significant at those levels of turbulence: for the upper curve it gives the contribution of order of 10% between 25 and 35 μm .

The system (6,7) is our mean-field model where the only memory of spatial inhomogeneities are the fallout term and the renormalization of the collision kernel K . As we show here, this model gives the rain initiation times with reasonable quantitative values and proper qualitative behavior upon the change of parameters. Let us discuss first how t_* depends on n . Here, the most important feature is the existence of the minimum in the function $t_*(n)$. That can be explained by the competition between condensation and collisions. Increasing n one decreases a_* (the crossover size for which condensation time is comparable to the time of collisional growth) and thus decreases the time needed for droplet growth. This works until a_* is getting comparable to $a_c \simeq (M/n\rho_0)^{1/3}$. Indeed, when droplets grow comparable to a_c vapor depletion slows and then stops condensation. If one takes the initial concentration even larger so that $a_c < a_*$ then vapor depletion stops condensation earlier and collisions are slower for droplets of the smaller size a_c so that the overall time of droplet growth is getting larger. The concentration n_* that corresponds to the minimal time can be found from the (implicit) relation $a_c \simeq a_*$ which corresponds to

$$(M/n_*\rho_0)^{-1/3} K \left[(M/n_*\rho_0)^{1/3} \right] \simeq \kappa s \quad (8)$$

That tells that $n_* \propto M$ and if $K \propto a^\alpha$ then $n_* \propto s^{3/(1-\alpha)}$. One can argue that for small concentrations (generally for maritime clouds), $n < n_*$, times of condensation and collision stages are comparable. Therefore, t_* is a function of the product Ms . For a homogeneous kernel, $t_* \propto n^{-2/(2+\alpha)}(Ms)^{-\alpha/(2+\alpha)}$. For

large concentrations (generally for continental clouds), $n > n_*$, the rain initiation time is mainly determined by collisions so it is getting independent of the supersaturation and $t_* \propto n^{(\alpha-3)/3}M^{-\alpha/3}$.

By numerically solving (6,7) with both gravity and turbulence-induced collisions we obtain the rain initiation time (also defined by the maximum of d^2W/dt^2) as a function of the CCN concentration n for different values of the supersaturation s and the vapor content M . The grid of radii was approximately exponential at sizes that are much larger than the size of initial condensation nuclei (with 200 points in unit interval of natural logarithm). The condensation of vapor was taken into account by working on evolving grid of radii $a_i(t)$ keeping conserved the total mass of water in droplets and vapor. Collisions were modelled according to (5) described above. Note that the numerical scheme we employ here has an additional advantage (comparing to those described in Pruppacher and Klett, 1997; Berry and Reinhardt, 1974; Bott, 1998) of accounting simultaneously for condensation and collisions while respecting conservation laws. We used the time step $dt = 0.01 \text{ s}$ during the condensation phase, on a later stage (dominated by coalescence) $dt = 0.1 \text{ s}$ was enough. Those results are presented in Figure 9 for $L = 2 \text{ km}$ and $\lambda = 20 \text{ s}^{-1}$. The solitary point at the lower part corresponds to $M = 6 \text{ g} \cdot \text{m}^{-3}$, $s = 1/150$. The three solid lines correspond to $M = 3 \text{ g} \cdot \text{m}^{-3}$ while the three dashed lines to $M = 1.5 \text{ g} \cdot \text{m}^{-3}$. Inside the triplets, the lines differ by the values of the supersaturation, from bottom to top, $s = 1/75, 1/150, 1/300$. We see that indeed the graphs $t_*(n)$ all have minima. The position of the minimum is proportional to M as expected and approximately proportional to $s^{-1/2}$ which would correspond to $\alpha \simeq 7$ in this interval of sizes. We see that the left parts of different curves with the same product sM approach each other as n decreases. To the right of the minima, the curves with different s but the same M approach each other as n increases. That supports the previous conclusions on the respective roles of condensation and collisions in determining the rain initiation time.

4. Delaying rain by hygroscopic over-seeding

That the rain time is a non-monotonic function of the concentration of droplets may provide a partial explanation for the conflicting observations of the effect of hygroscopic seeding. By seeding clouds with hygroscopic aerosol particles one can vary the number of cloud condensation nuclei and thus the number of small droplets at the beginning of the cloud formation. It was observed that such seeding in some cases suppresses precipitation (see e.g. Rosenfeld et al 2001), while in other cases enhances and accelerates it (Cotton and Pielke,

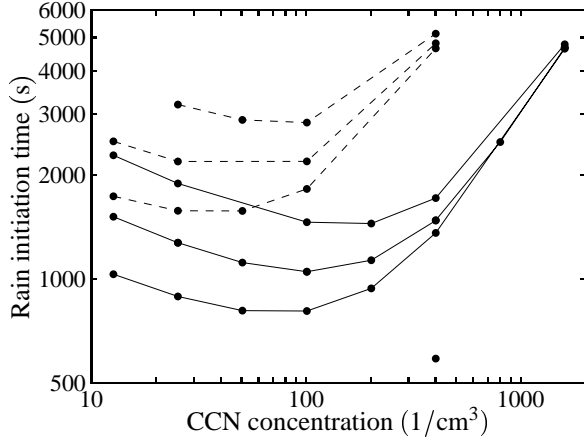


FIG. 9. Rain initiation time as function of CCN concentration n for different supersaturations s and vapor contents M .

1995; Mather 1991), see also Bruintjes (1999) for a recent review.

It is often desirable to postpone rain, for instance, to bring precipitation inland from the sea. The fact that t_* grows when $n > n_*$ suggests the idea of over-seeding to delay rain. This is considered to be unpractical: “It would be necessary to treat all portions of a target cloud because, once precipitation appeared anywhere in it, the raindrops ... would be circulated throughout the cloud ... by turbulence” (Dennis, 1980). We think that this conclusion ignores another, positive, aspect of cloud turbulence namely the mixing and homogenization of partially seeded cloud during the condensation stage. Let us describe briefly how it works for two cases.

Consider first seeding a part of the cloud comparable to its size L_c . Note that we do not consider here adding ultra-giant nuclei, we assume seeded CCN to be comparable in size to those naturally present. According to the Richardson law, the squared distance between two fluid parcels grows as ϵt^3 so that the rms difference of vapor concentrations between seeded and unseeded parts decreases as $t^{-9/4}$ when $t^3 > t_0^3 = L_c^2/\epsilon$ (ϵ is the energy dissipation rate in turbulence). To see how different rates of condensation interplay with turbulent mixing we generalize the mean-field system (6,7) describing seeded and unseeded parts by their respective n_1, n_2 and $x_1 = s_1 M_1, x_2 = s_2 M_2$ and link them by adding the term that models the decay of the difference: $dx_i/dt = \dots - (x_i - x_j)t(t + t_0)^{-2}(9/4)$. As a crude model, we assume two parts to evolve separately until $t = 2t_0$, then we treat the cloud as well-mixed and allow for the collisions between droplets from different parts. That actually underestimates the effect of seeding and can be considered as giving the lower bound for the time before rain. The results of simulations are

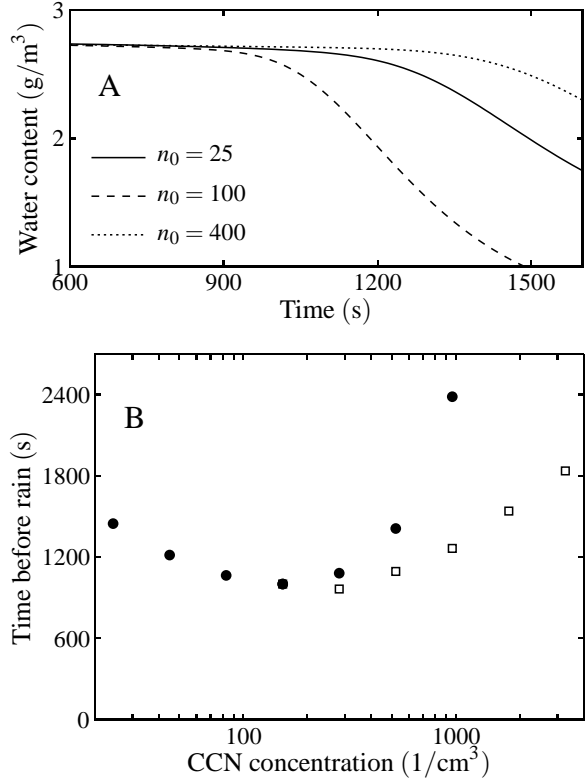


FIG. 10. Fraction of water left in the cloud as a function of time (A). Time of rain t_* as a function of CCN concentration n_0 (B). The lower part (boxes) corresponds to a half-seeded cloud (the half-sum of concentrations is used as abscissa).

shown in Fig. 10 for $t_0 = 180$ s, $L = 2$ km and $\lambda = 20$ s $^{-1}$. It is seen from Fig. 10A that the water content W changes similarly to what was shown in Figs. 2.3 and the rain initiation time is again determined by the maximum of d^2W/dt^2 . The respective times are shown against $n_0 = (n_1 + n_2)/2$ by boxes in Fig. 10B. The time increase is less than for homogeneous seeding but is still substantial. The fraction of the cloud still unmixed after the time t decreases by the Poisson law $\exp(-t/t_0)$. Taking $n_1 = 100$ cm $^{-3}$ one sees that for a time delay of 10 min one needs to seed by $n_2 \simeq 3000$ cm $^{-3}$.

Second, consider seeding by N particles a small part of the cloud which (unseeded) had some n_0 and would rain after t_* . After time t_* the seeds spread into the area of size $(\epsilon t_*^3)^{1/2}$ with the concentration inside the mixed region decaying as $n(t_*) = N(\epsilon t_*^3)^{-3/2}$ (for stratiform clouds one gets $N(\epsilon t_*^3)^{-1}$). To have an effect of seeding, one needs $n(t_*) > n_0$ which requires $N > 10^{15}$ for $n_0 = 50$ cm $^{-3}$, $t_* = 10$ min and $\epsilon = 10$ cm 2 s $^{-1}$. With sub-micron particles weighing 10^{-11} g that would mean hundreds of kilograms which is still practical.

5. Summary

We believe that our main result is a simple mean-field model (6,7) which demonstrates non-monotonic dependence of the rain initiation time on CCN concentration. As the CCN concentration increases, the rain initiation time first decreases and then grows as shown in Figs. 9,10. The simple modification of this model for an inhomogeneous case described in Sect. 4 shows that one can increase the rain initiation time even for a cloud partially seeded by hygroscopic aerosols.

We acknowledge support by the Ellentuck fund, by the Minerva and Israel Science Foundations and by NSF under agreement No. DMS-9729992. We are grateful to A. Khain, M. Pinsky and D. Rosenfeld for useful discussions.

REFERENCES

- Baker M.B, Corbin, R.G. and J. Latham: The effects of turbulent mixing in clouds. *Quart. J. Roy. Meteor. Soc.* **106**, 581.
- Berry, E. X. and R.L. Reinhardt, 1974: An analysis of cloud drop growth by collection. *J. Atm. Sci.* **31**, 1814–2127.
- Bott A, 1998: A flux method for the numerical solution of the stochastic collection equation *J. Atm.* **55**, 2284–2293.
- Beard KV, Durkee RI and Ochs HT. 2002: Coalescence efficiency measurements for minimally charged cloud drops, *J. Atm. Sci.* **59** 233–243.
- Bruintjes, R.T., 1999: A review of cloud seeding experiments to enhance precipitation and some new prospects, *Bull. Amer. Met. Soc.* **80**, 805–820.
- Cotton, W. R., and R. A. Pielke, 1995: *Human impacts on weather and climate*, (Cambridge Univ. Press, New York).
- Dennis, A. S. 1980: *Weather modification by cloud seeding* (Acad. Press, New York).
- Falkovich, G., A. Fouxon and M. G. Stepanov, 2002: Acceleration of rain initiation by cloud turbulence, *Nature* **419**, 151–154.
- Falkovich, G. and A. Pumir, 2004: Intermittent distribution of heavy particles in a turbulent flow. *Phys. Fluids* **16**, L47–50.
- Grits, B., M. Pinsky and A. Khain, 2000: Formation of small-scale droplet concentration inhomogeneity in a turbulent flow as seen from experiments with an isotropic turbulence model *Proc. 13th Int. Conf. on Clouds and Precipitation*.
- Gunn, R., and Kinzer, G. D. 1949: The terminal velocity of fall for water droplets in stagnant air. *J. Meteor.* **6**, 243.
- Jonas, P. 1996: Turbulence and cloud microphysics, *Atmos. Res.* **40**, 283–306.
- Korolev, A. 1995: The influence of supersaturation fluctuations on droplet size spectra formation, *J. Atm. Sci.* **52**, 3620–3634.
- Kostinski, A., and R. Shaw, 2001: Scale-dependent droplet clustering in turbulent clouds. *J. Fluid Mech.* **434**, 389–398.
- Mather, G. K. 1991: Coalescence enhancement in large multicell storms caused by the emissions from a Kraft paper mill, *J. Appl. Met.* **30**, 1134–1146.
- Maxey, M.R. 1987: The gravitational settling of aerosol particles in homogeneous turbulence and random flow field. *J. Fluid Mech.* **174**, 441–465.
- Pinsky, M., A. Khain and M. Shapiro, 2001: Collision efficiency of drops in a wide range of Reynolds numbers. *J. Atm. Sci.* **58**, 742–766.
- Pruppacher, H. R., and J. D. Klett, 1997: *Microphysics of Clouds and Precipitation* (Kluwer Acad. Publ., Dordrecht, ed. 2).
- Reade, W., and L. Collins, 2000: Effect of preferential concentration on turbulent collision rates. *Phys. Fluids* **12**, 2530–2540.
- Rosenfeld D., and G. Gutman, 1994: Retrieving microphysical properties near the tops of potential rain clouds by multispectral analysis of AVHRR data, *Atmos. Res.* **34**, 259–283.
- Rosenfeld, D., Y. Rudich and R. Lahav, 2001: Desert dust suppressing precipitation: A possible desertification feedback loop, *Proc. Nat. Ac. Sci. U.S.A.* **98**, 5975–5980.
- Saffman, P. and J. Turner, 1956: On the collision of drops in turbulent clouds, *J. Fluid Mech.* **1**, 16–30. ,
- Seinfeld, J. and S.Pandis, 1998: *Atmospheric Chemistry and Physics* (John Wiley and Sons, NY).
- Shaw, R. 2003: Particle-turbulence interaction in atmospheric clouds, *Ann. Rev. Fluid Mech.* **35**, 183–227. bibitem98SRCV Shaw, R., Reade, W., Collins, L. and J. Verlinde, 1998: Preferential concentration of cloud droplets by turbulence: effect on early evolution of cumulus cloud droplet spectra. *J. Atmos. Sci.* **55**, 1965–1976 (1998).
- Squires, K., and J. Eaton, 1991: Measurements of particle dispersion from direct numerical simulations of isotropic turbulence. *J. Fluid Mech.* **226**, 1–35.
- Sundaram, S., and L. Collins, 1997: Collision statistics in an isotropic particle-laden turbulent suspension, *J. Fluid Mech.* **335**, 75–109.
- Turitsyn, K., 2003: Air parcel random walk and droplet spectra broadening in clouds, *Phys. Rev. E* **67**, 062102.
- Vaillancourt, P.A., and M.K. Yau, 2000: Review of particle-turbulence interactions and consequences for cloud physics. *Bull. Amer. Met. Soc.* **81**, 285–298.
- van Dongen, P.G.J., and M.H. Ernst, 1988: Scaling solutions of Smoluchowski’s coagulation equation, *J. Stat. Phys.* **50** 295–328.
- Zakharov, V., V. Lvov and G. Falkovich, 1992: *Kolmogorov Spectra of Turbulence* (Springer-Verlag, Berlin)